Mice overexpressing CD97 in intestinal epithelial cells provide a unique model for mammalian postnatal intestinal cylindrical growth

Gabriela Aust[a], Christiane Kerner[a], Susann Gonsior[a], Doreen Sittig[a], Hartmut Schneider[b], Peter Buske[c], Markus Scholz[d], Norman Dietrich[a], Sindy Oldenburg[a], Olga N. Karpus[e], Jörg Galle[c], Salah Amasheh[f], and Jörg Hamann[e]

[a]Department of Surgery, Research Laboratories, [b]Department of Conservative Dentistry and Periodontology, [c]Interdisciplinary Center of Bioinformatics, and [d]Institute for Medical Informatics, Statistics and Epidemiology, University of Leipzig, 04103 Leipzig, Germany; [e]Department of Experimental Immunology, Academic Medical Center, University of Amsterdam, 1105 AZ Amsterdam, Netherlands; [f]Institute of Clinical Physiology, Charité, Campus Benjamin Franklin, 12203 Berlin, Germany

ABSTRACT **Postnatal enlargement of the mammalian intestine comprises cylindrical and luminal growth, associated with crypt fission and crypt/villus hyperplasia, respectively, which subsequently predominate before and after weaning. The bipartite adhesion G protein–coupled receptor CD97 shows an expression gradient along the crypt–villus axis in the normal human intestine. We here report that transgenic mice overexpressing CD97 in intestinal epithelial cells develop an upper megaintestine. Intestinal enlargement involves an increase in length and diameter but does not affect microscopic morphology, as typical for cylindrical growth. The megaintestine is acquired after birth and before weaning, independent of the genotype of the mother, excluding altered availability of milk constituents as driving factor. CD97 overexpression does not regulate intestinal growth factors, stem cell markers, and Wnt signaling, which contribute to epithelial differentiation and renewal, nor does it affect suckling-to-weaning transition. Consistent with augmented cylindrical growth, suckling but not adult transgenic mice show enlarged crypts and thus more crypt fissions caused by a transient increase of the crypt transit-amplifying zone. Intestinal enlargement by CD97 requires its seven-span transmembrane/cytoplasmic C-terminal fragment but not the N-terminal fragment binding partner CD55. In summary, ectopic expression of CD97 in intestinal epithelial cells provides a unique model for intestinal cylindrical growth occurring in breast-fed infants.**

Monitoring Editor
Thomas M. Magin
University of Leipzig

Received: Apr 3, 2013
Revised: May 6, 2013
Accepted: May 8, 2013

This article was published online ahead of print in MBoC in Press (http://www.molbiolcell.org/cgi/doi/10.1091/mbc.E13-04-0175) on May 15, 2013.

Study concept and design by G.A., acquisition of data by all authors, analysis and interpretation of data by G.A., C.K., S.A., and J.H., statistical analysis by G.A., drafting of the manuscript by G.A., critical revision of the manuscript for important intellectual content by J.H., and funding obtained by G.A. and S.A.

Address correspondence to: Gabriela Aust (gabriela.aust@medizin.uni-leipzig.de).

Abbreviations used: BrdU, bromodeoxyuridine; CTF, C-terminal fragment; GH, growth hormone; GLP, glucagon-like peptide; GPCR, G protein–coupled receptor; HE, hematoxylin-eosin; IGF, insulin-like growth factor; ISC, intestinal stem cell; Ko, knockout; Lgr, leucine-rich repeat-containing GPCR; NTF, N-terminal fragment; Tert, telomerase reverse transcriptase; Tg, transgenic; TM2, two-span transmembrane; TM7, seven-span transmembrane; WT, wild type.

INTRODUCTION

The generation of the mature mammalian intestinal tract entails dramatic morphological changes, yet the mechanisms that underlie intestinal growth after birth are largely obscure (Cummins and Thompson, 2002). Postnatal expansion of the epithelial surface of the small intestine occurs by two growth patterns known as cylindrical and luminal growth, respectively (Cummins and Thompson, 2002). In human infants, during milk feeding, cylindrical growth, comprising a gain in length and diameter without obvious microscopic morphological changes, predominates and peaks simultaneously with crypt fission, that is, the longitudinal division of crypts during the first year (Cummins *et al*., 2008). Thereafter crypt fission declines rapidly yet remains present at low level during adult life (Cummins and Thompson, 2002; Cummins *et al*., 2008). After weaning, luminal mucosal growth, characterized by crypt hyperplasia and a gain in submucosal folds and villi, becomes the dominant growth

pattern. Thus dietary transition at the end of the suckling period correlates with a change in intestinal growth pattern. Whether this change is the result of the dietary transition and/or changes in endogenous growth factors or is determined primarily by a genetic program switch during intestinal epithelial suckling-to-weaning transition and modulated secondarily by diet and/or growth factors is under debate (Cummins and Thompson, 2002; Harper *et al.*, 2011; Muncan *et al.*, 2011).

The adhesion class of G protein–coupled receptors (adhesion-GPCRs) comprises seven-span transmembrane (TM7) molecules with unusual long extracellular parts containing a juxtamembranous GPCR autoproteolysis-inducing domain (Langenhan *et al.*, 2013). This domain facilitates cleavage into an extracellular N-terminal fragment (NTF) and a TM7/cytoplasmic C-terminal fragment (CTF), which remain associated during expression at the cell surface (Lin *et al.*, 2004; Arac *et al.*, 2012). The NTF of adhesion-GPCRs can possess a variety of protein modules mediating cell and matrix interactions (Hamann *et al.*, 1995; Langenhan *et al.*, 2013). Adhesion-GPCRs are involved in developmental processes, including planar cell polarity (Usui *et al.*, 1999), tissue polarity (Langenhan *et al.*, 2009), neural development (Monk *et al.*, 2009; Boutin *et al.*, 2012), angiogenesis (Kuhnert *et al.*, 2010), and cardiogenesis (Waller-Evans *et al.*, 2010). How these functions are executed at the molecular level is poorly understood, essentially due to uncertainty about the role of the hitherto-identified adhesion-GPCR binding partners, the cooperation between the NTF and the CTF, and the downstream signaling pathways (Langenhan *et al.*, 2013).

CD97 is an adhesion-GPCR expressed by various normal cell types, including immune, epithelial, and muscle cells (Eichler *et al.*, 1994; Hamann *et al.*, 1995; Aust *et al.*, 1997; Steinert *et al.*, 2002). In the normal human intestine, CD97 is located in enterocytic cell–cell contacts, whereas gastrointestinal carcinomas strongly express CD97 in the membrane and the cytoplasm (Steinert *et al.*, 2002; Becker *et al.*, 2010). We previously reported that constitutive overexpression of CD97 in intestinal epithelial cells in transgenic (Tg) mice stabilizes membranous nonphosphorylated β-catenin, resulting in a strengthening of adherens junctions and an attenuation of experimental colitis (Becker *et al.*, 2010).

Unexpectedly, Tg(villin-CD97) mice develop an overt megaintestine phenotype, which we characterize here in detail. We show that massive enlargement of the upper intestine appears after birth and before weaning, yet with normal microscopic intestinal morphology, and coincides with enhanced crypt fission. Our data indicate that ectopic CD97 expression provides a unique model for enhanced cylindrical growth of the small intestine that we assign to the TM7/intracellular CTF of the receptor.

RESULTS

CD97 is expressed in crypt cells of the human small intestine

Immunohistochemical investigation of the human intestines revealed in normal colon a gradient in CD97 expression along the crypt axis, that is, CD97 was more expressed in lateral cell contacts of intestinal epithelial cells near the bottom of the crypt (Figure 1A). Similarly, in the small intestine, CD97 was present in the crypts, but expression became weaker along the crypt–villus axis (Figure 1B).

The intestinal expression pattern of CD97 in the mouse differs from that in humans (Veninga *et al.*, 2008). In immunostained sections, intestinal epithelial cells were nearly CD97 negative, whereas cells or extracellular matrix within the lamina propria mucosae expressed CD97, as in humans (Figure 1, C and D). In addition, in newborn and infant mice, we hardly found expression of CD97 in intestinal epithelial cells using immunohistology (data not shown). Of note, we found that a small number of crypt cells stain blue in a CD97 LacZ knock-in mouse model (Becker *et al.*, 2010). Thus the available tools provide no conclusive answer to the question of whether murine intestinal epithelial cells express CD97. Technically, this is not trivial, because other cell types present in the intestine, such as smooth muscle cells, fibroblasts, and leucocytes, are CD97 positive.

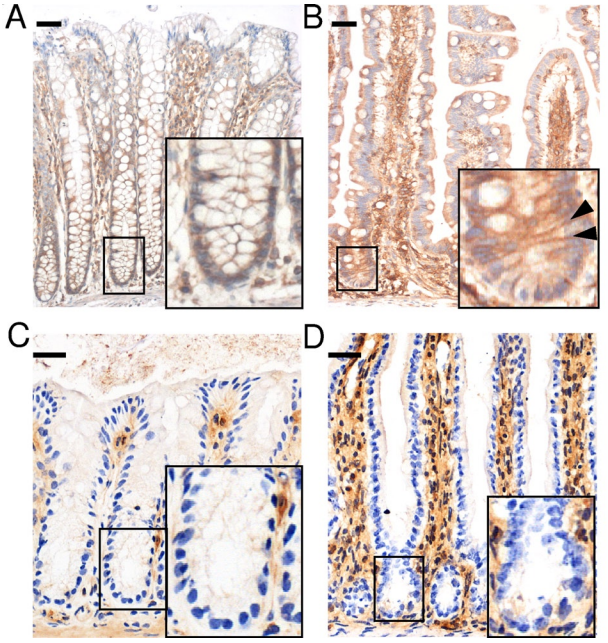

FIGURE 1: CD97 is located in lateral cell contacts of crypt cells in human CD97 and shows a gradient in expression along the crypt in the colon (A) and the crypt–villus axis in the small intestine (B). In crypt cells, CD97 is located mainly in lateral cell contacts (arrowheads; scale bar, 50 μm). In the murine colon (C) and small intestine (D), CD97 is not present in immunostained intestinal epithelial cells (2-wk-old mouse; scale bar, 25 μm).

We therefore applied a transgenic mouse model to investigate the significance of CD97 expression in epithelial cells (Becker *et al.*, 2010).

Overexpression of CD97 results in a megaintestine, with increased length and diameter of the upper small bowel

The villin promoter drives gene expression in immature and differentiated intestinal epithelial cells (Maunoury *et al.*, 1988). We previously generated three lines of Tg(villin-CD97) mice with increasing transgene copy number, designated Tg1, Tg2, and Tg3 (Becker *et al.*, 2010). Owing to poor reproduction, Tg3 was eventually lost, allowing only an initial intestinal assessment of this line.

Macroscopic inspection of adult animals revealed a significant increase in length and weight of the small intestine in Tg2 and Tg3 compared with wild-type (WT) mice (Figure 2, B and C). Whereas WT mice had small intestines with a length of 40.0 ± 0.4 cm and a weight of 1.19 ± 0.03 g, the small intestines of Tg2 and Tg3 mice were 48.3 ± 0.4 and 53.9 ± 0.8 cm in length and 2.13 ± 0.03 and 3.32 ± 0.03 g in weight (all $p < 0.001$), respectively. The megaintestine phenotype correlated with a transgene copy number of 10–15 in Tg1, 70–80 in Tg2, and ~400 in Tg3 (Becker *et al.*, 2010). Although in Tg2, changes were restricted to the small bowel and colon length and weight were unchanged, Tg3 mice also developed

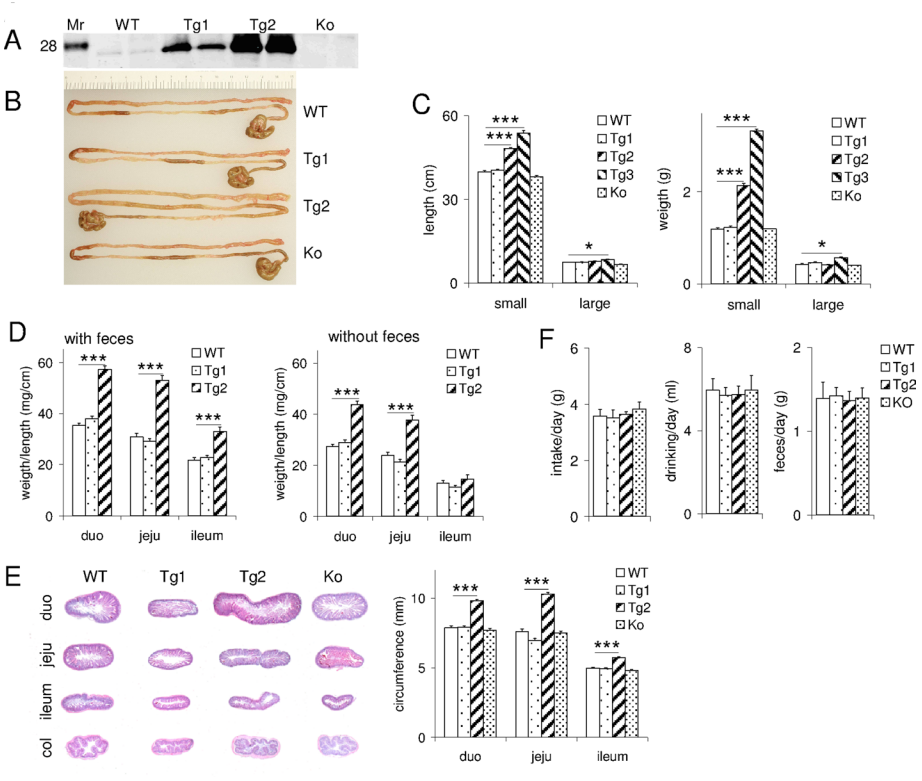

FIGURE 2: Tg(villin-CD97) mice develop megaintestine. (A) CD97 protein expression in lysates of the small intestine of two WT, Tg1, Tg2, and CD97Ko mice analyzed by Western blotting using an antibody directed to the CTF of CD97 (Mr, molecular weight marker). (B) Pictures taken from freshly prepared small intestine and cecum of several mouse strains show the increase in length of the small bowel in Tg2 mice. (C) Length and weight of the small intestine increased in adult Tg2 and Tg3 mice (Tg3, $n = 6$; other strains, $n = 16$; mean ± SEM; *$p < 0.05$, ***$p < 0.001$). (D) The increase in weight concerned all segments of the small bowel but was more pronounced in the duodenum (duo) and jejunum (jeju). Differences were independent of feces content (***$p < 0.001$). (E) Cross-sectional diameter increased in all segments of the small bowel in Tg2 mice (***$p < 0.001$). (F) Daily food intake and drinking ad libitum and the quantity of feces were comparable between mouse strains ($n = 10$/strain).

a longer colon (8.50 ± 0.18 cm) compared with WT mice (7.41 ± 0.15 cm; $p < 0.05$), suggesting that at very high copy number, CD97 overexpression also affects the large bowel. Figure 2A shows CD97 Western blot analysis of intestinal lysates, and Figure 2B shows pictures taken from the small intestine and the cecum of WT, Tg1, Tg2, and CD97 knockout (Ko) mice.

Intestinal enlargement in Tg2 mice involved all three segments of the small bowel but was more pronounced in the duodenum and jejunum and independent of feces content (Figure 2D). Morphometric analysis revealed an increase in diameter in each segment of the small bowel (Figure 2E). Food and water intake at random per day was comparable between WT and Tg mice, as was the amount of feces (Figure 2F).

CD97 overexpression does not affect intestinal microscopic morphology in adult mice

We next analyzed the small intestine of adult Tg2 mice at the microscopic level. We found no differences in 1) the thickness of the tissue layers, that is, muscosa, submucosa, and muscularis (data not shown); 2) the density, shape, length, and width of the villi (Figure 3A) and the depth and width of the crypts (Figure 3B); 3) the number of crypts feeding a single villus, the number and pattern of villi and crypts per area, and the percentage of crypt fissions (Figure 3C); 4) the length and width of intestinal epithelial cells and thus the number of epithelial cells/villus (data not shown); 5) the commitment of multipotential resorptive and secretory precursor cells, as can be concluded from mRNA levels of intestinal enzymes necessary for the digestion of high-fat-rich milk or solid carbohydrate-rich diet (Figure 3D), the number and position of Paneth, goblet, and enteroendocrine cells (Figure 3E and data not shown); and 6) the number and position of bromodeoxyuridine ($BrdU^+$) and active capase-3^+ enterocytes (Figure 3F and data not shown) along the crypt–villus axis. Thus the increase in length and diameter of the small intestine in adult Tg2 mice was not associated with changes in morphology or cell composition.

Intestinal enlargement in Tg(villin-CD97) mice occurs after birth and before weaning as an intrinsic trait

Newborn Tg2 mice showed the same length and weight of the small intestine as WT animals. Between weeks 2 and 3 after birth, Tg2 mice started to gain in small intestine length and weight that continued to increase (Figure 4A) without affecting the total body weight (Figure 4B).

Because the enlargement of the small intestine during lactation depends on growth factors in the milk such as lactoferrin (Zhang *et al.*, 2001; Cummins and Thompson, 2002; Liao *et al.*, 2012), we tested whether these factors caused the megaintestine phenotype in Tg(villin-CD97) mice. This possibility could be excluded because only Tg2 but not WT pups, derived from Tg2 females and WT males, developed a megaintestine (Figure 4C). Moreover, Tg2 pups from WT females and Tg2 males also showed a gain in length and weight of the small intestine (data not shown). In agreement, no obvious differences in the relative amount of major milk proteins, including lactoferrin, were found in Tg2 mice (Figure 4D). Finally, we examined whether expression of the lactoferrin receptor is increased in Tg2 mice. We confirmed highest levels of lactoferrin receptor mRNA in the small intestine (Suzuki and Lonnerdal, 2004) but found no changes in expression in infant Tg2 mice (Figure 4E).

During suckling, the epithelium expresses enzymes to digest fat-rich milk. We found no differences in the expression and time course of mRNAs of these enzymes between Tg2 and WT mice (Figure 3D). Argininosuccinate synthetase 1, necessary for the de novo synthesis of arginine absent in milk, and β-galactosidase, indispensable for the absorption of intact milk macromolecules, were expressed at high levels postnatally and down-regulated toward the end of the suckling period. In parallel, sucrase isomaltase and trehalase, which are involved in carbohydrate processing and required to digest solid diet, were up-regulated during the suckling-to-weaning transition.

Systemic or local growth factors such as growth hormone (GH), insulin-like growth factor 1 (IGF-1), IGF-2, and glucagon-like peptide 2 (GLP-2) stimulate intestinal growth (Ulshen *et al.*, 1993; Ohneda

et al., 1997; Lovshin *et al.*, 2000; Cummins and Thompson, 2002). Their circulating levels peak partly in the postnatal period, at which intestinal growth is most significant. In infant Tg2 mice, serum levels of IGF-1, IGF-2, and GLP-2 were not enhanced (Figure 5A). In line with this, mRNA levels of these factors and their receptors (Figure 5, B and C) and the percentage and position of the GLP-2$^+$ cells (Figure 5D) were not changed in the intestine of infant and adult Tg2 mice. Moreover, serum GH, measured at fixed time points to exclude effects from diurnal fluctuation (Sinha *et al.*, 1977), did not vary between infant and adult Tg2 and WT mice (Figure 5E). We conclude that the megaintestine in Tg(villin-CD97) mice develops during the suckling period, independent of the availability milk-derived and intrinsic growth factors and digestive enzymes.

Crypt fission and enterocyte proliferation are transiently enhanced in infant Tg(villin-CD97) mice

Next we carefully examined various intestinal morphometric parameters in infant Tg2 mice. The thickness of the different tissue layers and the shape, length, and width of the villi were comparable to those of WT animals (Figure 6, A and B). We found an increase, however, in the depth and width of the crypts in Tg2 mice (Figure 6, C and D). Crypt width, determined in the duodenum and jejunum, showed a normal distribution in WT mice, whereas in Tg2 mice, the mean crypt width was greater, and a notable increase in the number of very large crypts was seen (Figure 6E). These enlarged crypts were crypts immediately before or during fission (Figure 6F). The percentage of crypt fissions was fourfold higher in Tg2 than with WT mice, although the number of crypts and the crypt/villus ratio did not vary (Figure 6F).

In the small but not the large intestine of infant Tg2 mice, the number of proliferating intestinal epithelial cells was increased 2 h and, markedly, 24 h after BrdU application (Figure 7, A and B). Determination of the position of BrdU$^+$ cells along the crypt–villus axis confirmed this observation (Figure 7C). CD97 overexpression increases the crypt zone, which contains highly proliferative cells in the transit from the stem cell region to the villi called transit-amplifying cells (Potten, 1998; Crosnier *et al.*, 2006). In terms of the prospective fate they are not stem cells: all their progeny will differentiate and die (Crosnier *et al.*, 2006). Of interest, this increase was transient because in adult mice, no difference in the number and position of BrdU$^+$ cells between WT and Tg2 was seen (Figure 3F).

Intrinsic factors driving differentiation and continuous renewal of intestinal epithelium are normally present in Tg(villin-CD97) mice

Intestinal enlargement during the first postnatal weeks is accompanied by increased expression of intestinal stem cell (ISC) markers (Dehmer *et al.*, 2011). Quantification of mRNA to the ISC markers leucine-rich repeat-containing GPCR 5 (Lgr5), olfactomedin 4 (Olfm4), and telomerase reverse transcriptase (Tert) confirmed, in part, their higher expression in infant compared with adult mice but did not reveal a difference between Tg2 and WT animals (Figure 8A). Moreover, cell fate decisions, shown here exemplarily for the number and position of goblet cells, were not altered by CD97 overexpression in infant and adult Tg2 mice (Figure 8B and data not shown).

The Wnt pathway plays a pivotal role in proliferation and differentiation of intestinal epithelial cells. We previously demonstrated stabilization of nonphosphorylated β-catenin in the intestine of Tg(villin-CD97) mice that was not translocated to the nucleus (Becker *et al.*, 2010). In line with this, mRNA levels of the Wnt target genes axin-2, ephrin B3, and CD44 (Figure 8C) and nuclear localization of β-catenin in crypts of the small intestine (Figure 8D) were not changed in infant and adult Tg2 mice. In conclusion, enterocyte proliferation and crypt fission are transiently enhanced in Tg(villin-CD97) mice independent of ISC marker expression, cell fate decision, and Wnt pathway activity.

These data were confirmed by microarray analysis in which we identified 7074 genes to be expressed in mice jejunum of 2.5-wk-old mice. A total of 201 transcripts were differentially expressed with a fold change of >2 between WT and Tg2 (Supplemental Table S1). Of these, 95 showed down- and 106 showed up-regulation in Tg2 compared with WT mice. Kyoto Encyclopedia of Genes and Genomes (KEGG) pathway-enrichment analysis revealed that neither the Wnt (contains $n = 1$ of the differentially expressed transcripts) nor the Notch ($n = 0$) or Hedgehog ($n = 0$) signaling pathway, all involved in epithelial differentiation and continuous renewal (van den Brink *et al.*, 2004; Fre *et al.*, 2005; Kim *et al.*, 2005; van Es *et al.*, 2005; Cervantes *et al.*, 2009; van Dop *et al.*, 2009; Yamada *et al.*, 2010), were enriched. In the pathway Cell cycle, only one transcript was altered. Significant enrichments of differentially expressed genes were found in metabolic pathways as Drug metabolism/Metabolism of xenobiotics by cytochrome P450 ($n = 8$), Retinol metabolism ($n = 6$), and Fatty acid metabolism ($n = 5$). These metabolic pathways comprised, in part, the same transcripts, for example, for alcohol dehydrogenases and glutathione *S*-transferases, and analysis of differentially expressed genes with a fold change of >3 revealed no significant gene enrichment in any pathway. Thus, in infant Tg2 and WT jejunum, changes in global gene expression were small. Whether these alterations indeed result in an additional intestinal enlargement must be shown in future experiments.

Regulation of intestinal growth depends on the C-terminal fragment of CD97

Adhesion-GPCRs are two-subunit molecules with an adhesive NTF and a signaling CTF. Because evidence suggests that the fragments might function as separate entities (Langenhan *et al.*, 2013), we studied the contribution of the TM7/intracellular CTF to the megaintestine phenotype. Tg(villin-CD97/two-span transmembrane [TM2]) mice were generated that overexpress a CD97 receptor with only the first two membrane-spanning helices (Figure 9A). Six independent founders were identified (Figure 9B), giving rise to the lines TgTM2/1–6. In all lines, intestinal epithelial cells overexpressed CD97 (Figure 9C). The relative copy number of the CD97 transgene in the genome was calculated. TgTM2/1, 2, and 5 mice had integrated a number of CD97 cDNA copies that was equal to or higher than the number with the Tg2 strain (Figure 9D). Nonetheless, none of the TgTM2 lines developed a megaintestine (Figure 9E), indicating that the CTF of CD97 was necessary for induction of the megaintestine phenotype.

To study the role of CD97-mediated cell adhesion in development of the megaintestine, we crossed Tg(villin-CD97) mice with mice lacking CD55, a binding partner of CD97 that is present at low levels in enterocytes (Koretz *et al.*, 1992; Hamann *et al.*, 1996). Adult Tg2 × CD55 Ko mice developed a megaintestine that was indistinguishable from the phenotype in Tg2 mice, indicating that CD55 binding is not required for megaintestine induction (Figure 9F).

DISCUSSION

We report here that ectopic expression of CD97 in intestinal epithelial cells causes a massive enlargement of the small intestine without affecting microscopic morphology, multiple enterocytic cell lineage decisions, epithelial renewal, and suckling-to-weaning transition. The phenotype of the Tg(villin-CD97) mouse is unique compared

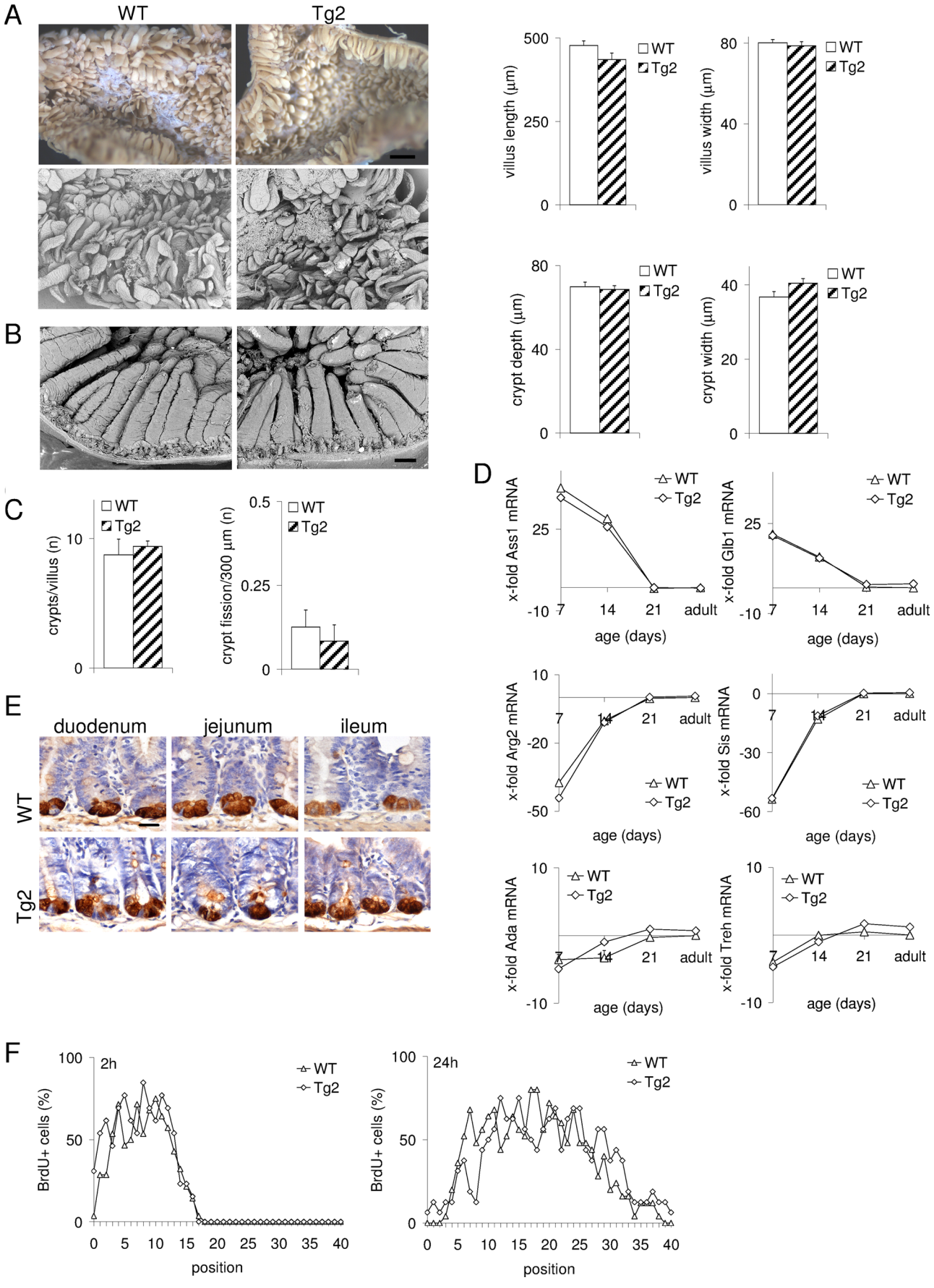
A
WT
Tg2
B
C
crypts/villus (n)
crypt fission/300 µm (n)
WT
Tg2
D
villus length (µm)
villus width (µm)
crypt depth (µm)
crypt width (µm)
x-fold Ass1 mRNA
x-fold Glb1 mRNA
x-fold Arg2 mRNA
x-fold Sis mRNA
x-fold Ada mRNA
x-fold Treh mRNA
age (days)
adult
E
duodenum
jejunum
ileum
F
2h
24h
BrdU+ cells (%)
position

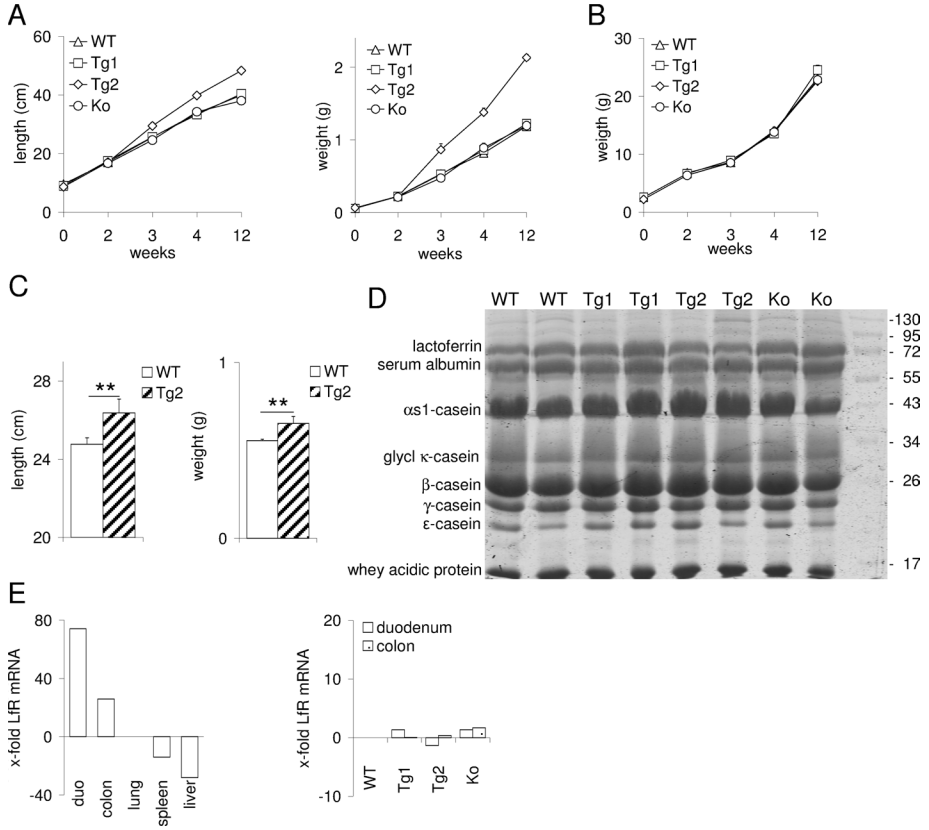

FIGURE 4: The megaintestine phenotype in Tg(villin-CD97) mice develops postnatally before weaning. (A) At the age of 3 wk, Tg2 mice started to gain in length and weight of the small intestine ($n = 10$/strain, mean ± SEM). (B) Body weight of Tg2 was comparable to that of the other mice ($n = 10$/strain). (C) Tg2 females were crossed with WT males. Only Tg2 offspring showed gain in weight and length of the small bowel ($n = 4$ litters with 15–20 pups/strain, $^{**}p < 0.01$). (D) Major milk proteins, such as lactoferrin, albumin, several caseins, and whey acidic protein, examined by SDS–PAGE were not different between Tg2, WT, Tg1, and CD97Ko at day 10 of lactation. (E) The small intestine showed the highest relative expression of lactoferrin receptor (LfR) mRNA compared with other tissues (left; normalized to lung). In 3-wk-old Tg2 mice, LfR mRNA levels in the duodenum and colon were not altered (right; $n = 4$ mice/strain; normalized to WT).

with existing megaintestine models, in which alteration of intestinal size is often accompanied by dramatic morphological changes (Ohneda *et al.*, 1997; Lovshin *et al.*, 2000; Zhang *et al.*, 2001; Lelievre *et al.*, 2007; Tamura *et al.*, 2008; Cervantes *et al.*, 2009; Langlois *et al.*, 2009; Lussier *et al.*, 2010; Yamada *et al.*, 2010). Acquisition of the megaintestine occurred after birth and before weaning and was associated with an increase in the crypt transit-amplifying zone, and thus crypt size and fission during this period. Owing to these characteristics, the Tg(villin-CD97) mouse provides a specific in vivo model for cylindrical intestinal growth, the dominant growth pattern in breast-fed infants.

Short-bowel resection in mice, in which 50% of the small intestine is surgically removed, induces an increase of the absorptive intestinal surface, primarily due to luminal mucosal growth (Helmrath *et al.*, 1996). It resembles regeneration in the small bowel syndrome seen in patients after extensive resection of the small intestine (Helmrath *et al.*, 1996; Thompson *et al.*, 2012). In mice and patients, the intestinal remnants increase nutrient absorption through structural changes, such as villous cell hyperplasia and dilation, and through functional mechanisms, such as increased mucosal enzyme activity and reduction of intestinal transit time (Thompson *et al.*, 2012). We observed none of these changes in Tg(villin-CD97) mice, fairly excluding contribution of luminal growth to the megaintestine phenotype. The Tg(villin-CD97) mice thus could be useful to understand and potentially activate cylindrical growth in patients with congenital or acquired small bowel syndrome.

How is CD97 involved in intestinal size control? The transient increase in enterocytic proliferation suggests a mitogenic effect of CD97. According to in silico simulations using an individual cell-based model of the intestinal crypt (Buske *et al.*, 2011), such an effect is sufficient to increase crypt size, which inevitably results in enhanced crypt fission. Nevertheless, this effect is surprising because 1) gene expression analysis revealed no alterations in the Cell cycle pathway and only moderate changes in global gene activity and 2) CD97 overexpression (Galle *et al.*, 2006) and siRNA knockdown (www.mitocheck.org) did not alter proliferation in tumor cells. So the questions remain about how this effect is induced by CD97 and why is it confined to the suckling period.

FIGURE 3: Adult Tg(villin-CD97) mice 14 wk of age have a normal intestinal microscopic morphology. (A) Stereo and raster electron micrographs reveal no differences in size, shape, and density of the villi in the duodenum of Tg2 mice. Luminal views are provided of wet-fixed samples (top; scale bar, 0.5 mm) and dried samples (bottom; scale bar, 0.2 mm). Right, morphometric analysis of HE-stained sections ($n = 6$ mice/strain; mean ± SEM). (B) The depth and width of the crypts are unchanged in adult Tg2 mice. Raster electron micrographs (left; scale bar, 0.1 mm) and morphometric analysis of HE-stained sections of the duodenum (right; $n = 6$ mice/strain). (C) The number of crypts that feed one villus and the number of crypt fissions are the same in Tg2 mice, as shown here for the duodenum ($n = 4$ mice/strain). (D) Duodenal mRNA levels of intestinal enzymes (Ada, adenosine deaminase; Arg2, arginase 2; Ass1, argininosuccinate synthetase 1; Glb1, β-galactosidase; Sis, sucrase isomaltase; Treh, trehalase) in Tg2 and WT mice at early life and adulthood are not different. RSP29 normalized $\log_2$ *x*-fold mRNA levels of several mouse groups compared with that of adult WT mice, which were set to 1 ($n = 3$ mice/group, mean ± SEM). (E) The number and position of Paneth cells, stained for lysozyme, was comparable in all segments of the small bowel of Tg2 mice (scale bar, 20 μm). (F) Determination of the position of $BrdU^+$ cells along the crypt–villus axis of the duodenum at 2 and 24 h after BrdU incorporation revealed no changes in Tg2 mice ($n = 6$/strain; on average, four crypt–villus structures per mouse were counted).

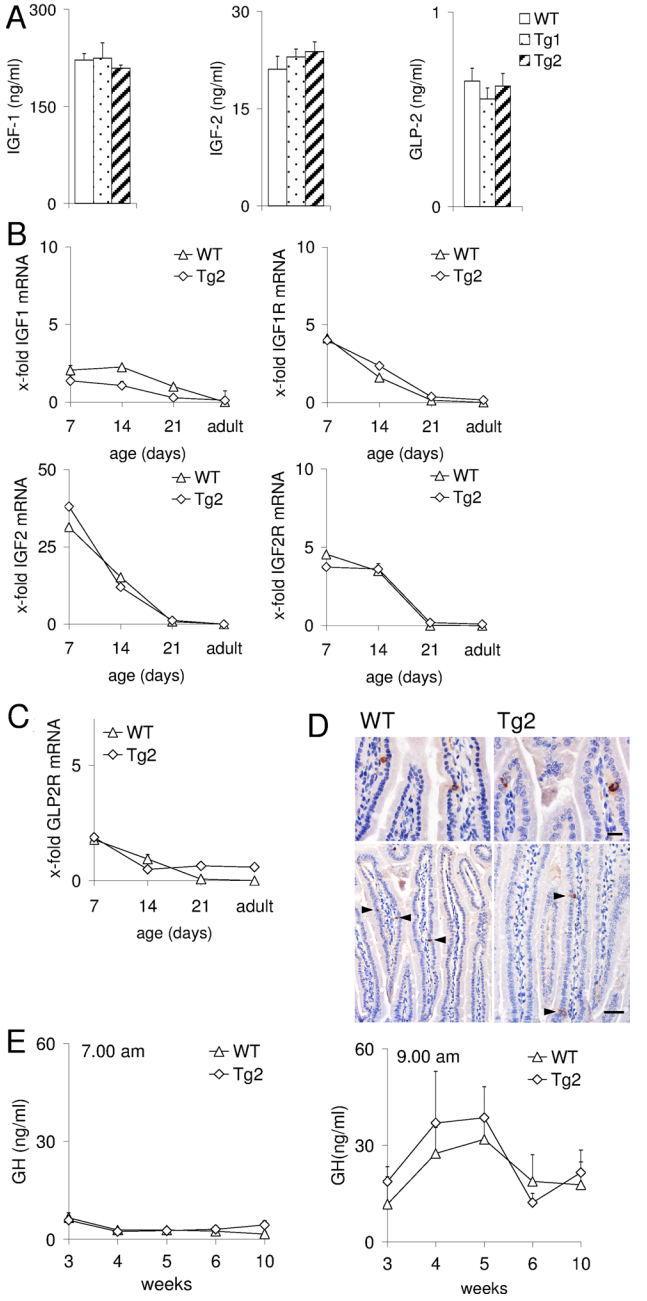

FIGURE 5: No change of several growth factors and their receptors in Tg2 mice. (A) Circulating IGF-1, IGF-2, and GLP-2 levels were comparable in 3-wk-old mice of the various strains (n = 10/strain, mean ± SEM). (B, C) Duodenal mRNA levels of IGF-1, IGF-2, their receptors (IGF-1/2R), and the GLP2 receptor (GLP-2R) were not different in Tg2 and WT mice at early life and adulthood. RSP29 normalized $\log_2$ x-fold mRNA levels of several mouse groups compared with that of adult WT mice, which were set to 1 (n = 3 mice/group, mean ± SEM). (D) Staining for GLP-2 revealed the same number and position of these rare enteroendocrine cells in the duodenum of 3-wk-old WT and Tg2 mice (scale bar, top, 20 µm; bottom, 50 µm). (E) Circulating GH determined at fixed time points (7.00–7.30 and 9.00–9.30 am for low and high GH levels, respectively) did not vary between infant and adult WT and Tg2 mice (n = 10/strain; mean ± SEM).

We first hypothesized that CD97 induces the megaintestine by regulating molecules known to change growth behavior and determine the size of the small intestine, such as 1) transiently available trophic or endogenous growth factors and/or their receptors, 2) modulators of ISCs, and 3) regulators of the Wnt pathway.

1. CD97 overexpression may regulate a temporally available growth factor in the milk, such as lactoferrin, or its receptor (Liao *et al.*, 2012). We found that suckling Tg2 but not WT pups developed a megaintestine phenotype independent of the genotype of the mother, thus excluding this possibility. Moreover, we showed that lactoferrin receptor mRNA levels were unchanged in Tg2 mice. Next to milk constituents, circulating and intestinal endogenous growth factors promote intestinal enlargement. Enhanced availability of these factors causes significant alterations in intestinal microscopic morphology, suggesting promotion of primarily intestinal luminal growth (Ulshen *et al.*, 1993; Ohneda *et al.*, 1997; Lovshin *et al.*, 2000; Cummins and Thompson, 2002; Lelievre *et al.*, 2007). We found no changes in several growth factors and their receptors in Tg2 mice. Nevertheless, we cannot exclude at this point that CD97 regulates the binding or signaling of a receptor for a (milk) growth factor in the small intestine during breastfeeding.
2. ISCs residing at the base of the crypts, quiescent in the 4+ position, directly above the Paneth cells, or as crypt base columnar cells scattered between them, are responsible for the differentiation and continuous renewal of intestinal epithelial cells (Umar, 2010). This activity persists throughout life at a stable level, which contrasts notably with intestinal cylindrical growth that peaks during infancy and declines rapidly thereafter. Whether the recently described increase in ISC marker expression during intestinal growth (Dehmer *et al.*, 2011) suggests that ISCs drive intestinal cylindrical growth remains to be shown. Although we found an increase in BrdU incorporation in crypt cells and in crypt fission in infant Tg2 mice, mRNA expression of the ISC markers Lgr5, Tert, and Olfm4 was not enhanced.
3. Activation of the Wnt cascade such as through Wnt5a/Ror2 or R-spondin regulates morphogenesis of the small intestine prenatally and postnatally (Kim *et al.*, 2005; Cervantes *et al.*, 2009; Yamada *et al.*, 2010). In Tg(villin-CD97) mice, the gain in intestinal size was not associated with increased Wnt signaling. The percentage of crypt cells with nuclear localization of β-catenin and the mRNA levels of Wnt target genes were not increased in infant and adult Tg2 mice, confirming our previous finding that CD97 overexpression stabilizes nonphosphorylated membrane-bound and cytosolic β-catenin but does not cause its translocation to the nucleus (Becker *et al.*, 2010). This finding was confirmed additionally by genome-wide expression analysis. Regulation of the Wnt, Notch, and Hedgehog pathways, all involved in epithelial differentiation and continuous renewal (van den Brink *et al.*, 2004; Fre *et al.*, 2005; Kim *et al.*, 2005; van Es *et al.*, 2005; Cervantes *et al.*, 2009; van Dop *et al.*, 2009; Yamada *et al.*, 2010), by CD97 overexpression seems to be unlikely.

Ruling out several growth factors, stem cell numbers, and Wnt activity as the origin of the transient CD97-induced mitogenic effect, we are investigating two other scenarios. First, proteins located in lateral epithelial cell junctions possess functions related to controlling intestinal size after birth. The best evidence comes from claudin-15–deficient and, to a lesser extent, claudin-2–deficient mice, which grow normally with an enlarged upper small intestine (Tamura *et al.*, 2008, 2011). In contrast to our transgenic mice, the megaintestine in these mice developed after weaning and correlated with massive morphological changes such as are typical for luminal intestinal growth (Tamura *et al.*, 2008). In the normal human intestine and in

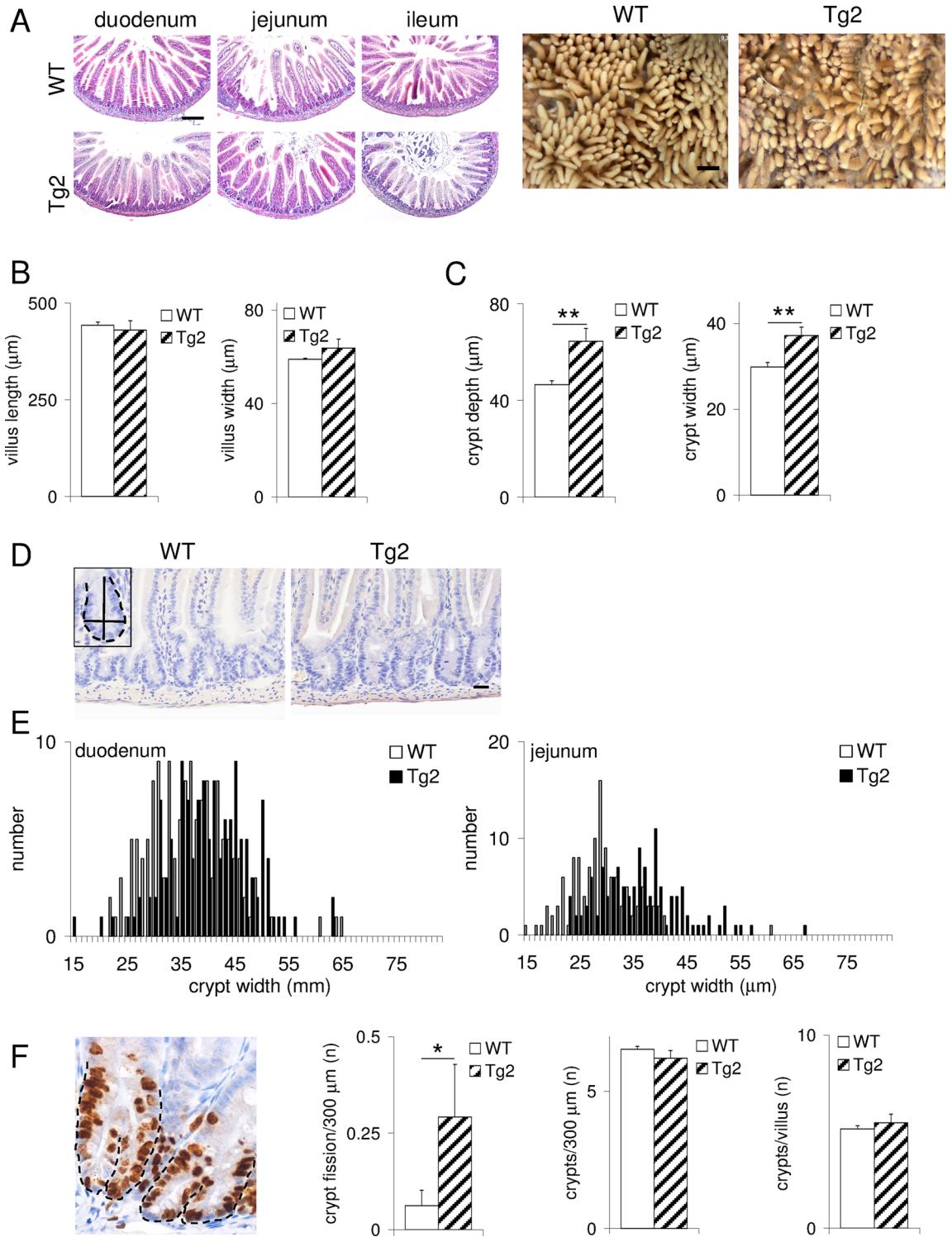

FIGURE 6: The percentage of crypt fission is increased In 3-wk-old infant Tg(villin-CD97) mice. (A) In Tg2 and WT mice, the microscopic morphology of the small intestine was comparable, as seen in HE cross-sections (left) and in stereo micrographs of the duodenum (right; scale bar, 0.2 mm). (B, C) The depth and width of the crypts was increased, whereas the length and width of the villi was unchanged in the duodenum of 3-wk-old Tg2 mice (6 mice/strain; mean ± SEM; $^{**}p < 0.01$). (D) In infant Tg2 mice, enlarged crypts were seen. The detail shows how depth and width of a crypt were measured (hematoxylin; scale bar, 25 µm). (E) The crypt width (duodenum, $n = 150$; ileum, $n = 125$ crypts/strain counted) was normally distributed in WT but not Tg2 mice. In Tg2 mice, the width of all crypts and especially of enlarged crypts in fission was increased. (F) The number of crypts in fission was increased in Tg2 mice, whereas the number of crypts/area was unchanged compared with WT ($n = 6$ mice/strain; $^{*}p < 0.05$). Analysis of serial HE-stained villi and crypt cross-sections revealed no changes in the number of crypts that feed one villus ($n = 5$ mice/strain). Two fissioning crypts in the duodenum of a Tg2 mouse are shown as examples in the micrograph. Nuclei were stained for BrdU incorporation for 2 h and counterstained with hematoxylin.

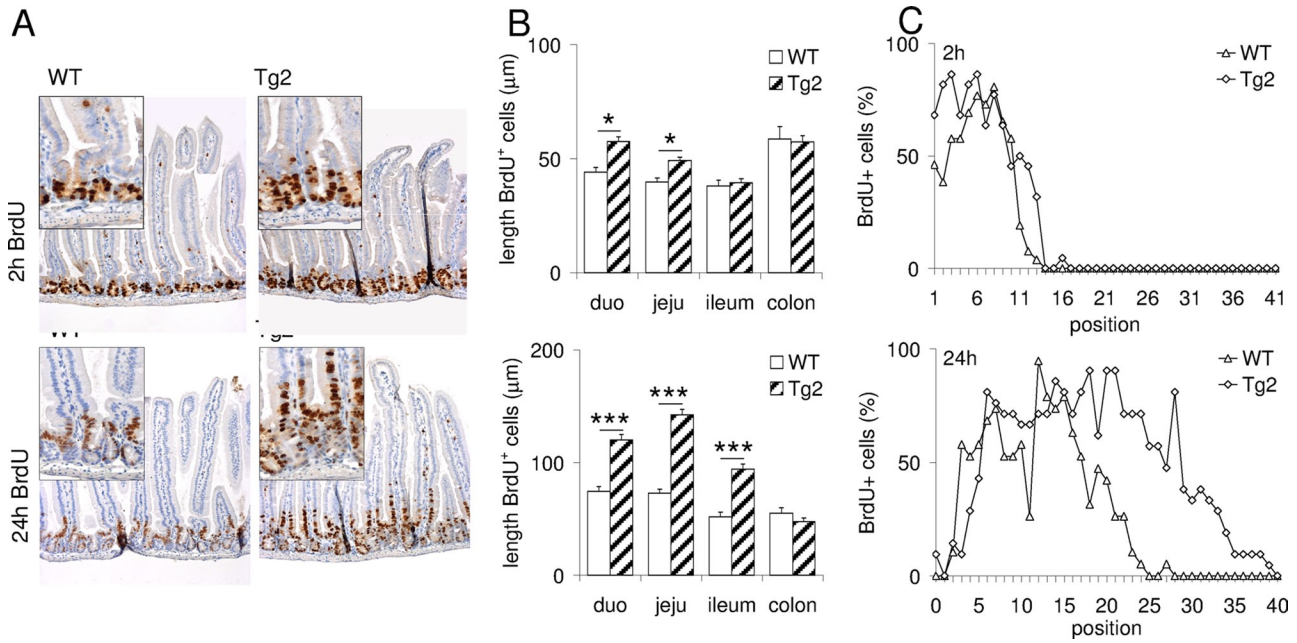

FIGURE 7: Increased intestinal proliferation in 3-wk-old Tg(villin-CD97) mice. (A, B) The length of the proliferating zone was increased in all segments of the small intestine but not the colon of Tg2 mice ($n = 6$/strain; mean ± SEM; $^*p < 0.05$, $^{***}p < 0.001$) at 2 and 24 h after BrdU incorporation. Shown here is the duodenum. (C) Determination of the position of BrdU$^+$ cells along the crypt–villus axis of the duodenum 2 and 24 h after BrdU incorporation ($n = 6$/strain; on average, four crypt–villus structures/mouse were counted).

Tg(villin-CD97) mice CD97 is located in adherens junctions, which are strengthened by CD97 (Becker *et al.*, 2010). Thus intestinal overexpression of CD97 modulates the regulation of adherens junctions and intestinal growth simultaneously, yet a causative relationship, if one exists, remains to be established.

Second, there is increasing evidence that developmental and differentiation processes are controlled by chromatin modifiers as shown recently for ISCs (Benoit *et al.*, 2012). Crypts contain two physically distinct proliferative compartments—the stem cell zone and the transit-amplifying zone, which is located in the middle of the crypt containing the fast-growing and differentiating transit cells (Potten, 1998; Crosnier *et al.*, 2006). The increase in the BrdU$^+$ crypt zone and thus crypt size in suckling Tg(villin-CD97) mice suggests that CD97 overexpression increases this transit-amplifying zone perhaps by interfering with chromatin modifiers such as the polycomb repressive complex 2 (Benoit *et al.*, 2012). Changes in chromatin modifier activity would not necessarily change microscopic morphology as in the relation between the absorptive and the secretory cell lineages or villus size. However, how an increase in the transit-amplifying zone may result in a cylindrical intestinal enlargement remains unexplained.

Our data provide new insights into signaling of adhesion-GPCRs (Langenhan *et al.*, 2013). Typically for these receptors, CD97 consists of an extracellular NTF and a TM7/cytoplasmic CTF (Hamann *et al.*, 1995; Gray *et al.*, 1996). We recently described a role of CD97 in susceptibility to experimental arthritis and granulopoiesis, which correspond to very similar phenotypes in mice lacking CD55, suggesting a role of the CD97–CD55 interaction in leukocyte adherence (Hoek *et al.*, 2010; Veninga *et al.*, 2011). In the present study we did not find this phenocopy. CD55 Ko mice have a normal intestine, that is, development of the megaintestine in Tg(villin-CD97) mice does not require the presence of the ligand CD55. In marked contrast, intestinal enlargement requires the presence of 7TM/intracellular CTF. Our study strengthens the hypothesis that the NTF and CTF of adhesion-GPCRs might execute separate functions, related to cell adhesion and signaling (Langenhan *et al.*, 2013).

In summary, the adhesion-GPCR CD97 can markedly enhance intestinal enlargement within the limited time period of predominant cylindrical growth, correlating with the suckling period. It should be noted that intestinal cylindrical growth, that is, a gain of length and diameter and thus the area of the intestine, requires a parallel expansion of the deeper intestinal layers, such as the submucosa, muscularis, and serosa. CD97 overexpression in the intestinal epithelium is sufficient to induce an enlargement of all intestinal layers, without obvious morphological changes. Thus Tg(villin-CD97) mice provide a unique model with which to study and understand mechanisms and molecules underlying cylindrical growth of the small intestine and the inducer role of epithelial cells in this process in breast-fed infants.

MATERIALS AND METHODS

Ethics statement

This research complied with the ethics guidelines of the University of Leipzig and the Academic Medical Center, Amsterdam. For the generation of transgenic mice and for animal experiments, we obtained ethics approval from the Landesdirektion Leipzig (TVV16/11) and the Academic Medical Center, Amsterdam (DSK10044-175). Human intestinal samples were studied with approval from the Ethics Committee of the Medical Faculty of the University of Leipzig (028/2000, 111/2009). Written consent was obtained from all study participants.

Transgenic mice

The generation of Tg(villin-CD97) mice, expressing full-length mouse CD97(EGF1,2,3,4) under control of the villin promoter, has been described (Becker *et al.*, 2010). Tg(villin-CD97/TM2) mice, expressing CD97(EGF1,2,3,4) with only the first two of the seven transmembrane

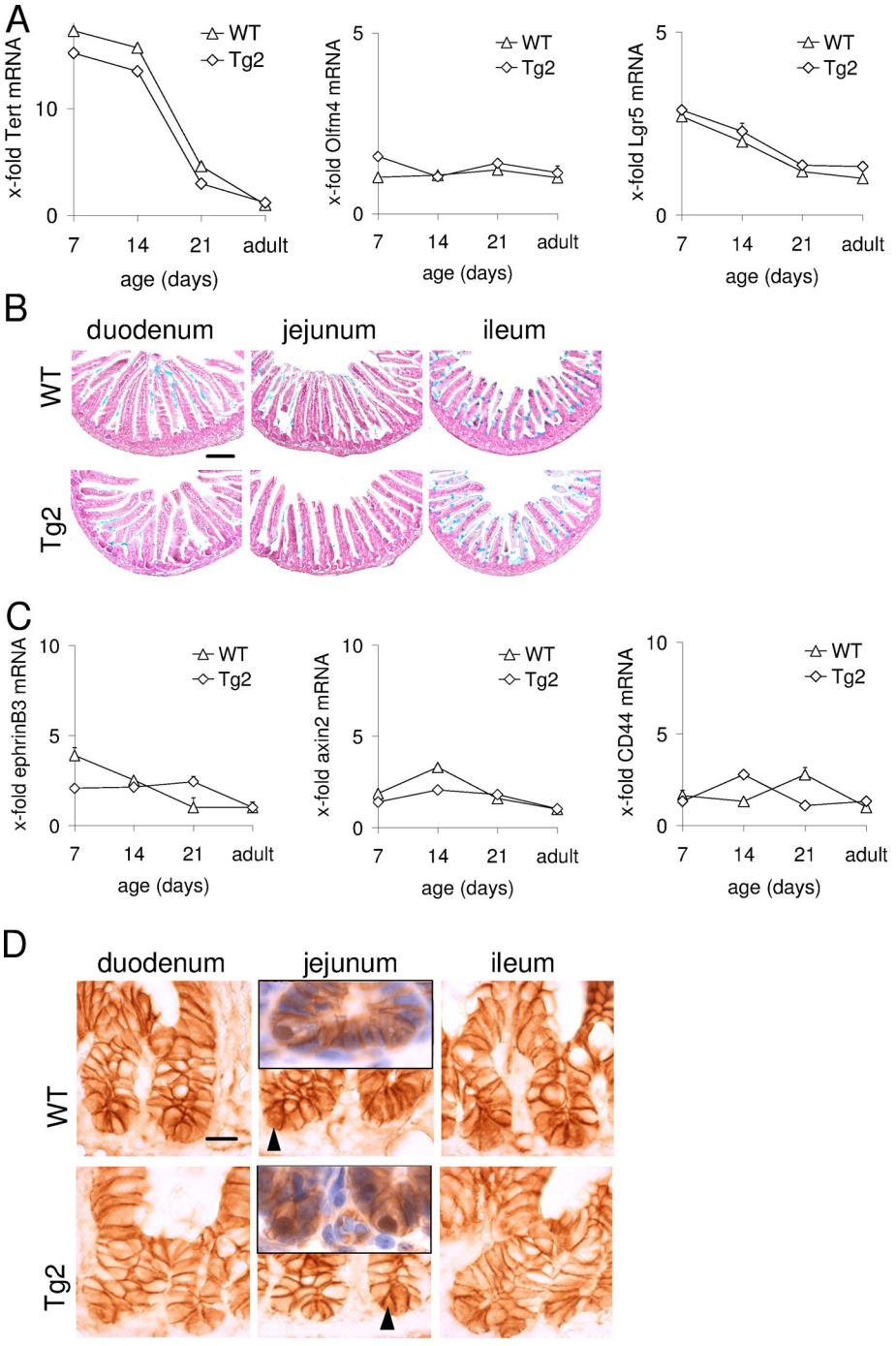

FIGURE 8: CD97 does not alter cell fate decision, β-catenin localization, and mRNA levels of Wnt target genes. (A) mRNA levels of ISC markers in Tg2 and WT mice at early life and adulthood were not different. Olfm4 and Lgr5 as markers of crypt base columnar cells and Tert as a marker for position 4+ ISC were quantified by real-time PCR. RSP29 normalized $\log_2$ *x*-fold mRNA levels of the ISC marker gene of several mouse groups compared with that of adult WT mice, which were set to 1 ($n = 3$ mice/group, mean ± SEM). (B) Alcian blue/neutral red staining revealed the same number and position of goblet cells in the various parts of the small intestine of infant 2.5-wk-old Tg2 and WT mice (scale bar, 0.15 mm). (C) mRNA levels of Wnt target genes known to be up-regulated by nuclear β-catenin were quantified by real-time PCR in adult mice. RSP29-normalized $\log_2$ *x*-fold mRNA levels of ephrin B3, axin-2, and CD44 compared with WT mice ($n = 3$ mice/group; mean ± SEM). (D) Intracellular localization of β-catenin in infant 2.5-wk-old Tg2 and WT mice was examined by immunohistology (scale bar, 10 μm). Only a few crypt epithelial cells with faint nuclear β-catenin staining, most likely Paneth cells, were seen in both strains (arrowheads). Inserts show costaining for β-catenin and HE.

helices and without the intracellular C-terminus, were generated by a comparable approach. The expression construct was created by placing a 9-kb regulatory region of the villin gene upstream of a CD97(EGF1,2,3,4) cDNA, truncated behind Val-583. The CD97(EGF1,2,3,4/TM2) cDNA was amplified from a pcDNA3.1/Zeo(+)-mCD97(EGF1,2,3,4) construct (Hamann *et al.*, 2000), using the primer pair 5′-ccgcgtacggccaccatgaggagcgtc-3′/5′-tgtcacgcgtcacgccgaccaggaatatgat-3′, and subcloned via *Bsi*WI and *Mlu*I into a pBS-KS-Villin-MES-SV40-polyA plasmid (Pinto *et al.*, 1999), kindly provided by S. Robine (Institute Curie, Paris, France). Tg(villin-CD97/TM2) mice were generated by pronuclear microinjection as described (Becker *et al.*, 2010). Founders were screened by amplification of the transgene using primers 5′-tgccttctcctctaggctcgt-3′/5′-gtcctgcacatggtactgag-3′, generating a 1500–base pair PCR product. To establish Tg(villin-CD97/TM2) lines, founders were mated to C57BL/6J WT mice (Charles River, Sulzfeld, Germany). Six transgenic lines were obtained. The relative copy number of the integrated CD97 cDNA in these lines was calculated by real-time PCR.

CD97 Ko mice were generated before (Veninga *et al.*, 2008). Tg(villin-CD97) × CD55 Ko mice were derived by crossing Tg2 with CD55 Ko mice (Lin *et al.*, 2001), kindly provided by M. E. Medof (Case Western Reserve University, Cleveland, OH). All mice were crossed back on a C57BL/6J background, and WT littermates were used as controls. Mice were housed under specific pathogen-free conditions.

Food and water intake and defecation

Food and water intake and defecation were measured daily for 4 d in metabolic cages (Ehret, Emmendingen, Germany). Food intake was determined by weighing the metal cage top, including the food. Deionized water was available from a 50-ml bottle with 0.2-ml gradations. Feces was collected daily and weighed. Body weight was measured at the beginning and end of the 4-d test.

Milk proteins

Milk was collected at midlactation 10 d after birth. Dams separated from their pups 2 h before were injected with 0.2 U of synthetic oxytocin (Hexal, Holzkirchen, Germany) and then anesthetized. Approximately 70 μl of milk was collected. Milk was diluted 1:3 with Aqua Dest, skimmed by centrifugation (4000 × *g*, 15 min), and separated by SDS–PAGE. Milk proteins were visualized by Coomassie blue staining.

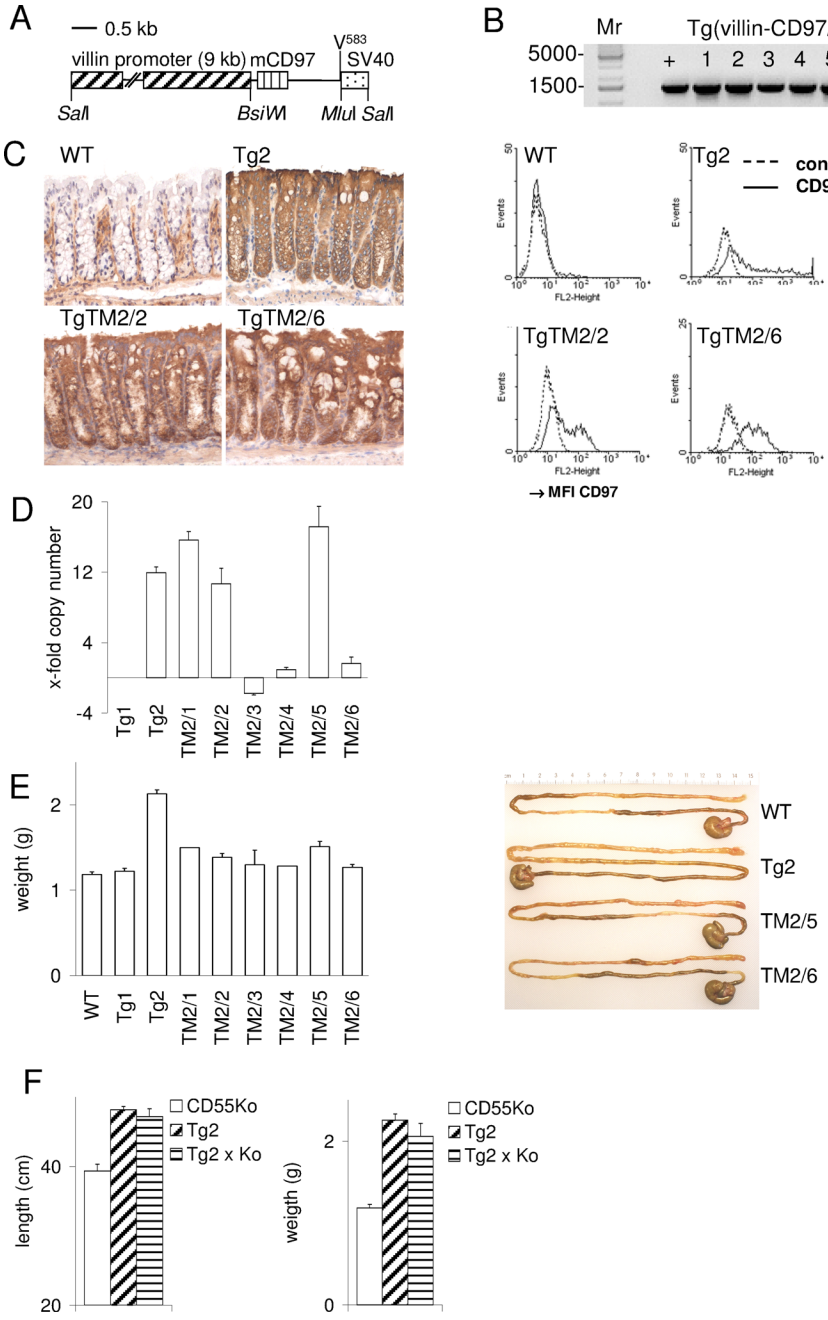

FIGURE 9: Tg(villin-CD97/TM2) mice do not develop a megaintestine. (A) Schematic representation of the pBS-KS-villin-CD97 construct, showing the villin promoter (hatched box), the mCD97 cDNA containing EGF-like domains 1–4, and the SV40 polyadenylation sequence (dotted box). (B) PCR of gDNA confirmed integration of the CD97 transgene in six founders. (C) CD97 immunostaining of colonic tissue of WT, Tg2, TgTM2/2, and TgTM2/6 mice revealed that in WT colon only cells of the lamina propria mucosae were stained, whereas in transgenic mice the enterocytes were strongly CD97$^+$. Flow cytometry revealed expression of truncated CD97 at the surface of enterocytes in TgTM2 mice. (D) The integrated relative copy number of the CD97 transgene was measured by real-time PCR (normalized to Tg1). TgTM2/1, 2, and 5 integrated a CD97 cDNA copy number greater than or equal to that of the Tg2 mice. (E) Adult 14-wk-old TgTM2 mice did not develop a megaintestine. Shown here is the weight of the small intestine (TgTM2/1 and 4, $n = 2$; all other lines, $n > 5$ mice; mean ± SEM). Tg2 but not TgTM2 mice showed lengthening of the small intestine (right). (F) Tg2 was crossed to CD55 Ko mice. Adult 12-wk-old Tg2 × CD55 Ko mice developed a megaintestine phenotype ($n > 5$ mice/strain).

Serum levels of growth factors

IGF-1 and -2 were measured by radioimmunoassay by L. Pridzun (Mediagnost, Reutlingen, Germany). GLP-2 and GH were determined using enzyme-linked immunosorbent assay (Kamiya Biomedical Company, Seattle, WA, and Millipore, Schwalbach, Germany). Based on a diurnal profile of GH generated for 2- to 4-wk-old WT mice, daily measurements of low and high GH levels were performed in serum collected at 7:00–7:30 and 9:00–9:30 am, respectively.

Intestinal morphology

After scarification, the entire small intestine and the colon were weighed. The length of the small intestine was measured under uniform tension. The following segments were dissected: duodenum from the pylorus to the ligament of Treitz, proximal jejunum (first third of the intestine after the ligament of Treitz), and distal ileum (last third of the intestine up to the ileocecal valve). Each segment was weighed with and without feces. The diameter of the segments, the thickness of each intestinal layer, the length and width of the villi, and the depth and width of the crypts were measured in hematoxylin-eosin (HE)–stained sections under a light microscope using AxioVision program 4.8 (Carl Zeiss, Jena, Germany). The ratio of the number of crypts and villi per unit area was calculated in serial HE-stained villus and crypt cross-sections. The number of crypts and the percentage of crypt fissions were determined in longitudinal sections at 5 × 300–µm length of each intestinal segment. Paneth, enteroendocrine, and goblet cells were examined by immunostaining with polyclonal antibodies for lysozyme, chromogranin A (Dako, Hamburg, Germany), and GLP-2 (Santa Cruz Biotechnology, Heidelberg, Germany) and by Alcian blue/neutral red staining, respectively.

Pictures of the intestinal luminal surface were obtained from cleaned bowel segments fixed in 2.5% glutardialdehyde/phosphate-buffered saline (PBS) for 24 h, using a stereo light microscope (Stemi 2000; Carl Zeiss). Afterward, specimens were cut, dehydrated, dried in a critical-point apparatus (Pelco CPD2; Ted Pella, Redding, CA), and examined with a scanning electron microscope (Phenom G2Pro; Phenom-World, Eindhoven, Netherlands).

Proliferation and apoptosis

We injected 2 mg/ml BrdU (Sigma-Aldrich, Munich, Germany)/PBS intraperitoneally (50 mg/kg body weight). Mice were killed 2 and 24 h after injection. In 5-µm paraffin sections, proliferating or apoptotic cells were detected by staining with the BrdU In-situ Detection Kit II (BD Biosciences, Heidelberg, Germany) or by staining active caspase-3 with an antibody recognizing its p17 subunit (R&D Systems, Wiesbaden,

Germany) overnight, followed by detection with the Vectastain Elite ABC Kit (Vector Laboratories, Burlingame, CA).

Gene expression

Relative gene expression levels were measured by real-time PCR using ABsolute qPCR Sybr Green Mix (Abgene, Epsom, United Kingdom) on a Rotor Gene 3000 thermal cycler (Qiagen, Hilden, Germany) with the *Ct* method (Pfaffl, 2001). Expression of specific genes was normalized to RPS29 (de Jonge *et al.*, 2007) as endogenous control, using the primers (forward/reverse) 5′-tgaaggcaagatgggtcac-3′/5′-gcacatgttcagcccgtatt-3′. Growth factors and their receptors were amplified using the primer pairs lactoferrin receptor 5′-caggtggggcaattctttcttttc-3′/5′-agttgtgcaggggggcttttgtt-3′, IGF-1 5′-tcatgtcgtcttcacacctcttct-3′/5′-ccacacacgaactgaagagcat-3′, IGF-1 receptor 5′-gtgggggctcgtgtttctc-3′/5′-gatcaccgtgcagtttc-3′, IGF-2 5′-acacttcgatttgaaccacattc-3′/5′-gagagctcaaaccatgcaaact-3′, IGF-2 receptor 5′-gggaagctgttgactccaaaa-3′/5′-gcagcccatagtggtgttgaa-3′, and GLP-2 receptor 5′-ccttccccatgctgtttgttattc-3′/5′-agcggcccca-ggtctttctca-3′. ISC markers were amplified using the primer pairs Lgr5 5′-ttcaccccaatgcgttttctac-3′/5′-gttgccgtcgtctttattccattg-3′, Olfm4 5′-ctctgcctcccggacaactct-3′/5′-gtcagcgggaaaggcggtatc-3′, and Tert 5′-gcccagcatttcacccagcgtctc-3′/5′-gcatcataggccccggtcacatc-3′. Wnt target genes were amplified with the primer pairs axin-2 5′-caggagcctcacccttcg-3′/5′-acgccgaggtgcttgccc-3′, ephrin B3 5′-aacagcttcccctgattgtg-3′/5′-gacccataatggaagcctca-3′, and CD44 5′-ggcagaagaaaaagctggtg-3′/5′-acaccccaatcttcatgtc-3′. Sucrase isomaltase, trehalase, adenosine deaminase, arginase 2, argininosuccinate synthetase 1, and β-galactosidase were amplified as described (Muncan *et al.*, 2011).

In addition, gene expression was quantified in the jejunum of 2.5-wk-old mice with the MouseRef-8 v2.0 Expression BeadChip (Illumina, San Diego, CA) comprising 25,697 features. A single array was used to measure RNA of two WT and two Tg2 mice with two biological replicates each ($n = 8$ samples in total). Array processing was performed using the recommendations of the manufacturer. Data were preprocessed on the basis of the nonnormalized, not–background-corrected outputs of GenomeStudio (Illumina). Transcripts were analyzed if detected in at least four samples with a detection p value of 0 and if the signal-to-noise ratio was ≥2. Transcripts were quantile normalized and log 2 transformed. In the statistical analysis, gene expressions of biological replicates were averaged. Expressions were compared between WT and Tg2 mice by calculating t tests and fold changes. Pathway-enrichment analysis was performed using DAVID (Huang *et al.*, 2009a,b).

CD97 expression

Quantification of CD97 at the surface of isolated intestinal epithelial cells, staining of CD97 in cryostat sections, and Western blotting using an antibody directed to the C-terminus of CD97 were performed as described (Veninga *et al.*, 2008; Becker *et al.*, 2010). For immunostaining of paraffin-embedded human tissues, 5-µm sections were rehydrated. Endogenous peroxidase was blocked with 1.0% H_2O_2/96% ethanol between the steps absolutely and 96% ethanol for 5 min. After antigen retrieval with citrate buffer, pH 6.0, the sections were incubated with a rabbit polyclonal antibody to CD97 (Sigma-Aldrich) for 30 min. Binding was detected with a biotin-labeled goat anti-rabbit secondary antibody for 30 min, followed by Vectastain Elite ABC Kit.

Statistical analysis

Statistical analysis was performed using the Student's t test or Mann–Whitney test; $p < 0.05$ was regarded as significant.

ACKNOWLEDGMENTS

The work was supported by grants from the German Research Foundation to G.A. (AU 132-7/1) and S.A. (AM 141/4-1). We thank Claudia Vogel, Claudia Rüger, and Niels Kamp for excellent technical assistance and Gijs van den Brink and Vanesa Muncan for helpful discussions.

REFERENCES

Arac D, Boucard AA, Bolliger MF, Nguyen J, Soltis SM, Sudhof TC, Brunger AT (2012). A novel evolutionarily conserved domain of cell-adhesion GPCRs mediates autoproteolysis. EMBO J 31, 1364–1378.

Aust G, Eichler W, Laue S, Lehmann I, Heldin N-E, Lotz O, Scherbaum WA, Dralle H, Hoang-Vu C (1997). CD97: a dedifferentiation marker in human thyroid carcinomas. Cancer Res 57, 1798–1806.

Becker S, Wandel E, Wobus M, Schneider R, Amasheh S, Sittig D, Kerner C, Naumann R, Hamann J, Aust G (2010). Overexpression of CD97 in intestinal epithelial cells of transgenic mice attenuates colitis by strengthening adherens junctions. PLoS One 5, e8507.

Benoit YD, Lepage MB, Khalfaoui T, Tremblay E, Basora N, Carrier JC, Gudas LJ, Beaulieu JF (2012). Polycomb repressive complex 2 impedes intestinal cell terminal differentiation. J Cell Sci 125, 3454–3463.

Boutin C, Goffinet AM, Tissir F (2012). Celsr1–3 cadherins in PCP and brain development. Curr Top Dev Biol 101, 161–183.

Buske P, Galle J, Barker N, Aust G, Clevers H, Loeffler M (2011). A comprehensive model of the spatio-temporal stem cell and tissue organisation in the intestinal crypt. PLoS Comput Biol 7, e1001045.

Cervantes S, Yamaguchi TP, Hebrok M (2009). Wnt5a is essential for intestinal elongation in mice. Dev Biol 326, 285–294.

Crosnier C, Stamataki D, Lewis J (2006). Organizing cell renewal in the intestine: stem cells, signals and combinatorial control. Nat Rev Genet 7, 349–359.

Cummins AG, Catto-Smith AG, Cameron DJ, Couper RT, Davidson GP, Day AS, Hammond PD, Moore DJ, Thompson FM (2008). Crypt fission peaks early during infancy and crypt hyperplasia broadly peaks during infancy and childhood in the small intestine of humans. J Pediatr Gastroenterol Nutr 47, 153–157.

Cummins AG, Thompson FM (2002). Effect of breast milk and weaning on epithelial growth of the small intestine in humans. Gut 51, 748–754.

de Jonge HJ, Fehrmann RS, de Bont ES, Hofstra RM, Gerbens F, Kamps WA, de Vries EG, van der Zee AG, te Meerman GJ, ter Elst A (2007). Evidence based selection of housekeeping genes. PLoS One 2, e898.

Dehmer JJ, Garrison AP, Speck KE, Dekaney CM, Van LL, Sun X, Henning SJ, Helmrath MA (2011). Expansion of intestinal epithelial stem cells during murine development. PLoS One 6, e27070.

Eichler W, Aust G, Hamann D (1994). Characterization of the early activation-dependent antigen on lymphocytes defined by the monoclonal antibody BL-Ac(F2). Scand J Immunol 39, 111–115.

Fre S, Huyghe M, Mourikis P, Robine S, Louvard D, Artavanis-Tsakonas S (2005). Notch signals control the fate of immature progenitor cells in the intestine. Nature 435, 964–968.

Galle J, Sittig D, Hanisch I, Wobus M, Wandel E, Loeffler M, Aust G (2006). Individual cell-based models of tumor–environment interactions. Multiple effects of CD97 on tumor invasion. Am J Pathol 169, 1802–1811.

Gray JX, Haino M, Roth MJ, Maguire JE, Jensen PN, Yarme A, Stetler-Stevenson MA, Siebenlist U, Kelly K (1996). CD97 is a processed, seven-transmembrane, heterodimeric receptor associated with inflammation. J Immunol 157, 5438–5447.

Hamann J, Eichler W, Hamann D, Kerstens HM, Poddighe PJ, Hoovers JM, Hartmann E, Strauss M, van Lier RA (1995). Expression cloning and chromosomal mapping of the leukocyte activation antigen CD97, a new seven-span transmembrane molecule of the secretion receptor superfamily with an unusual extracellular domain. J Immunol 155, 1942–1950.

Hamann J, van Zeventer C, Bijl A, Molenaar C, Tesselaar K, van Lier RA (2000). Molecular cloning and characterization of mouse CD97. Int Immunol 12, 439–448.

Hamann J, Vogel B, van Schijndel GM, van Lier RA (1996). The seven-span transmembrane receptor CD97 has a cellular ligand (CD55, DAF). J Exp Med 184, 1185–1189.

Harper J, Mould A, Andrews RM, Bikoff EK, Robertson EJ (2011). The transcriptional repressor Blimp1/Prdm1 regulates postnatal

reprogramming of intestinal enterocytes. Proc Natl Acad Sci USA 108, 10585–10590.
Helmrath MA, VanderKolk WE, Can G, Erwin CR, Warner BW (1996). Intestinal adaptation following massive small bowel resection in the mouse. J Am Coll Surg 183, 441–449.
Hoek RM, de LD, Kop EN, Yilmaz-Elis AS, Lin F, Reedquist KA, Verbeek JS, Medof ME, Tak PP, Hamann J (2010). Deletion of either CD55 or CD97 ameliorates arthritis in mouse models. Arthritis Rheum 62, 1036–1042.
Huang D-W, Sherman BT, Lempicki RA (2009a). Bioinformatics enrichment tools: paths toward the comprehensive functional analysis of large gene lists. Nucleic Acids Res 37, 1–13.
Huang D-W, Sherman BT, Lempicki RA (2009b). Systematic and integrative analysis of large gene lists using DAVID bioinformatics resources. Nat Protoc 4, 44–57.
Kim KA *et al.* (2005). Mitogenic influence of human R-spondin1 on the intestinal epithelium. Science 309, 1256–1259.
Koretz K, Bruderlein S, Henne C, Moller P (1992). Decay-accelerating factor (DAF, CD55) in normal colorectal mucosa, adenomas and carcinomas. Br J Cancer 66, 810–814.
Kuhnert F *et al.* (2010). Essential regulation of CNS angiogenesis by the orphan G protein-coupled receptor GPR124. Science 330, 985–989.
Langenhan T, Aust G, Hamann J ((2013). Sticky signaling—adhesion class G protein-coupled receptors take the stage. Sci Signal 6, re3.
Langenhan T *et al.* (2009). Latrophilin signaling links anterior-posterior tissue polarity and oriented cell divisions in the *C. elegans* embryo. Dev Cell 17, 494–504.
Langlois MJ, Roy SA, Auclair BA, Jones C, Boudreau F, Carrier JC, Rivard N, Perreault N (2009). Epithelial phosphatase and tensin homolog regulates intestinal architecture and secretory cell commitment and acts as a modifier gene in neoplasia. FASEB J 23, 1835–1844.
Lelievre V *et al.* (2007). Gastrointestinal dysfunction in mice with a targeted mutation in the gene encoding vasoactive intestinal polypeptide: a model for the study of intestinal ileus and Hirschsprung's disease. Peptides 28, 1688–1699.
Liao Y, Jiang R, Lonnerdal B (2012). Biochemical and molecular impacts of lactoferrin on small intestinal growth and development during early life. Biochem Cell Biol 90, 476–484.
Lin F, Fukuoka Y, Spicer A, Ohta R, Okada N, Harris CL, Emancipator SN, Medof ME (2001). Tissue distribution of products of the mouse decay-accelerating factor (DAF) genes. Exploitation of a Daf1 knockout mouse and site-specific monoclonal antibodies. Immunology 104, 215–225.
Lin HH, Chang GW, Davies JQ, Stacey M, Harris J, Gordon S (2004). Autocatalytic cleavage of the EMR2 receptor occurs at a conserved G protein-coupled receptor proteolytic site motif. J Biol Chem 279, 31823–31832.
Lovshin J, Yusta B, Iliopoulos I, Migirdicyan A, Dableh L, Brubaker PL, Drucker DJ (2000). Ontogeny of the glucagon-like peptide-2 receptor axis in the developing rat intestine. Endocrinology 141, 4194–4201.
Lussier CR, Brial F, Roy SA, Langlois MJ, Verdu EF, Rivard N, Perreault N, Boudreau F (2010). Loss of hepatocyte-nuclear-factor-1alpha impacts on adult mouse intestinal epithelial cell growth and cell lineages differentiation. PLoS One 5, e12378.
Maunoury R, Robine S, Pringault E, Huet C, Guenet JL, Gaillard JA, Louvard D (1988). Villin expression in the visceral endoderm and in the gut anlage during early mouse embryogenesis. EMBO J 7, 3321–3329.
Monk KR, Naylor SG, Glenn TD, Mercurio S, Perlin JR, Dominguez C, Moens CB, Talbot WS (2009). A G protein-coupled receptor is essential for Schwann cells to initiate myelination. Science 325, 1402–1405.
Muncan V *et al.* (2011). Blimp1 regulates the transition of neonatal to adult intestinal epithelium. Nat Commun 2, 452.
Ohneda K, Ulshen MH, Fuller CR, D'Ercole AJ, Lund PK (1997). Enhanced growth of small bowel in transgenic mice expressing human insulin-like growth factor I. Gastroenterology 112, 444–454.
Pfaffl MW (2001). A new mathematical model for relative quantification in real-time RT-PCR. Nucleic Acids Res 29, e45.
Pinto D, Robine S, Jaisser F, El Marjou FE, Louvard D (1999). Regulatory sequences of the mouse villin gene that efficiently drive transgenic expression in immature and differentiated epithelial cells of small and large intestines. J Biol Chem 274, 6476–6482.
Potten CS (1998). Stem cells in gastrointestinal epithelium: numbers, characteristics and death. Philos Trans R Soc Lond B Biol Sci 353, 821–830.
Sinha YN, Salocks CB, Wickes MA, Vanderlaan WP (1977). Serum and pituitary concentrations of prolactin and growth hormone in mice during a twenty-four hour period. Endocrinology 100, 786–791.
Steinert M, Wobus M, Boltze C, Schütz A, Wahlbuhl M, Hamann J, Aust G (2002). Expression and regulation of CD97 in colorectal carcinoma cell lines and tumor tissues. Am J Pathol 161, 1657–1667.
Suzuki YA, Lonnerdal B (2004). Baculovirus expression of mouse lactoferrin receptor and tissue distribution in the mouse. Biometals 17, 301–309.
Tamura A, Hayashi H, Imasato M, Yamazaki Y, Hagiwara A, Wada M, Noda T, Watanabe M, Suzuki Y, Tsukita S (2011). Loss of claudin-15, but not claudin-2, causes Na(+) deficiency and glucose malabsorption in mouse small intestine. Gastroenterology 140, 913–923.
Tamura A *et al.* (2008). Megaintestine in claudin-15-deficient mice. Gastroenterology 134, 523–534.
Thompson JS, Rochling FA, Weseman RA, Mercer DF (2012). Current management of short bowel syndrome. Curr Probl Surg 49, 52–115.
Ulshen MH, Dowling RH, Fuller CR, Zimmermann EM, Lund PK (1993). Enhanced growth of small bowel in transgenic mice overexpressing bovine growth hormone. Gastroenterology 104, 973–980.
Umar S (2010). Intestinal stem cells. Curr Gastroenterol Rep 12, 340–348.
Usui T, Shima Y, Shimada Y, Hirano S, Burgess RW, Schwarz TL, Takeichi M, Uemura T (1999). Flamingo, a seven-pass transmembrane cadherin, regulates planar cell polarity under the control of Frizzled. Cell 98, 585–595.
van den Brink GR *et al.* (2004). Indian Hedgehog is an antagonist of Wnt signaling in colonic epithelial cell differentiation. Nat Genet 36, 277–282.
van Dop WA *et al.* (2009). Depletion of the colonic epithelial precursor cell compartment upon conditional activation of the hedgehog pathway. Gastroenterology 136, 2195–2203.
van Es JH *et al.* (2005). Notch/gamma-secretase inhibition turns proliferative cells in intestinal crypts and adenomas into goblet cells. Nature 435, 959–963.
Veninga H *et al.* (2008). Analysis of CD97 expression and manipulation: antibody treatment but not gene targeting curtails granulocyte migration. J Immunol 181, 6574–6583.
Veninga H, Hoek RM, de Vos AF, de Bruin AM, An FQ, van der Poll T, van Lier RA, Medof ME, Hamann J (2011). A novel role for CD55 in granulocyte homeostasis and anti-bacterial host defense. PLoS One 6, e24431.
Waller-Evans H *et al.* (2010). The orphan adhesion-GPCR GPR126 is required for embryonic development in the mouse. PLoS One 5, e14047.
Yamada M, Udagawa J, Matsumoto A, Hashimoto R, Hatta T, Nishita M, Minami Y, Otani H (2010). Ror2 is required for midgut elongation during mouse development. Dev Dyn 239, 941–953.
Zhang P, Sawicki V, Lewis A, Hanson L, Nuijens JH, Neville MC (2001). Human lactoferrin in the milk of transgenic mice increases intestinal growth in ten-day-old suckling neonates. Adv Exp Med Biol 501, 107–113.